International Journal of Heat and Mass Transfer 70 (2014) 864–874

Contents lists available at ScienceDirect

International Journal of Heat and Mass Transfer

journal homepage: www.elsevier.com/locate/ijhmt

A coupled lattice Boltzmann and finite volume method for natural convection simulation

Zheng Li [a,b], Mo Yang [b], Yuwen Zhang [a,*]

[a] Department of Mechanical and Aerospace Engineering, University of Missouri, Columbia, MO 65211, USA
[b] College of Energy and Power Engineering, University of Shanghai for Science and Technology, Shanghai 200093, China

ARTICLE INFO

Article history:
Received 21 September 2013
Received in revised form 26 November 2013
Accepted 26 November 2013
Available online 20 December 2013

Keywords:
Nonequilibrium extrapolation scheme
Lattice Boltzmann method
Finite volume method
Natural convection

ABSTRACT

A coupled lattice Boltzmann and finite volume method is proposed to solve natural convection in a differentially heated squared enclosure. The computational domain is divided into two subdomains and a message passing zone is between them. The velocity and temperature fields are respectively solved using D2Q9 and D2Q5 models in lattice Boltzmann method (LBM) while SIMPLE algorithm is applied to the finite volume method (FVM). The velocity and temperature information transfers are fulfilled by a non-equilibrium extrapolation scheme. Pure FVM, pure LBM, and the coupled method with two different geometric settings are applied to solve the natural convection with different Rayleigh numbers. The results obtained from the coupled method agreed with those from pure FVM and LBM very well.

1. Introduction

The fluid flow and heat transfer problems encountered in engineering applications span into different scales and there are different numerical methods for different scales. Molecular dynamics (MD) [1] can be applied to solve nano- and microscale problems while lattice Boltzmann method (LBM) is a typical mesoscopic scale method [2]. Finite volume method (FVM), on the other hand, is suitable for solving the macroscale problems [3]. The growing multiscale problems must be solved with multiscale method since there is no method that is suitable for all the scales. There exist research works about the multiscale methods in the literature, e.g., MD-LBM [4–6], MD-FVM [7–9] and LBM-FVM [10–12].

There are several models for the fluid flow and heat transfer problems in LBM. He et al. proposed the internal energy function by relating internal energy with the kinetic energy of particle for the incompressible fluid flow and heat transfer [13]. Then its simplified thermal LBM model was advanced by Peng et al. [14] while Guo et al. introduced a coupled lattice BGK model based on Boussinesq assumption [15]. The D2Q9 and D2Q5 models were respectively used to solve the velocity and temperature fields [16]. Meanwhile, Semi-implicit Method for Pressure Linked Equation (SIMPLE) [17] is one of the most frequently used algorithms in FVM. The D2Q9 and D2Q5 model were respectively used to solve the velocity and temperature fields [16]. Meanwhile, Semi-Implicitly Method for Pressure Linked Equation (SIMPLE) [17] is one of the most frequently used algorithms in FVM.

The objective of this paper is to combine the LBM and FVM as a coupled method to solve the fluid flow and heat transfer problem. The total computational domain is divided into FVM and LBM zones with a message passing zone between them. So there is an artificial boundary for each sub-domain. It is necessary to obtain the artificial information from the other sub-domain to fulfill the coupled method. For the fluid flow and heat transfer simulation, the problems under consideration are described using the macroscopic variables, such as velocity, temperature, pressure and density. And these variables in LBM are based on the density and energy distributions results while they can be solved directly in FVM. Meanwhile macroscopic variables can be transferred from the density and energy distributions results directly. So it is quite straightforward to obtain the FVM artificial boundary information from the inner nodes in the LBM zone. But macroscopic variables are not enough to obtain the corresponding density and energy distributions results.

Latt [18] and Latt et al. [19] coupled LBM and finite difference method (FDM) for the pure fluid flow with the first-order expansion of the lattice Boltzmann equation. However, the FDM itself has the limitation when solving problems with complex computational domain [3]. This shortfall restricts the development of LBM-FDM because the one of the most attractive advantages of LBM is its suitability to solve the problems in complex computational domain. Luan et al. [20] solved natural convection using the LBM-FVM with the general reconstruction operator [21]and obtained persuasive results. However general reconstruction

* Corresponding author. Tel.: +1 5738846936.
E-mail address: zhangyu@missouri.edu (Y. Zhang).

0017-9310/$ - see front matter © 2013 Elsevier Ltd. All rights reserved.
http://dx.doi.org/10.1016/j.ijheatmasstransfer.2013.11.077

Nomenclature

c	lattice speed
c_s	speed of sound
$\boldsymbol{e}_i$	particle speed
F	body force
f_i	density distribution
$\boldsymbol{g}$	gravity acceleration (m/s^2)
$\boldsymbol{G}$	effective gravitational acceleration (m/s^2)
g_i	energy distribution
H	height of the cavity (m)
Ma	Mach number
Nu	Nusselt number
p	pressure (N/m^2)
P	nondimensional pressure
Pr	Prandtl number
Ra	Rayleigh number
t	time (s)
T	temperature (K)
u	horizontal velocity (m/s)
U	nondimensional horizontal velocity
v	vertical velocity (m/s)
V	nondimensional vertical velocity
$\boldsymbol{V}$	velocity

Greek Symbols

α	thermal diffusivity (m^2/s)
β	volume expansion coefficient of the fluid (K^{-1})
θ	nondimensional temperature
μ	viscosity (N s/m^2)
ν	kinematic viscosity (m^2/s)
ρ	density (kg/m^3)
τ	nondimensional time
τ_v	relaxation time for velocity
τ_T	relaxation time for energy
ω_i	value factor for velocity
ω_i^T	value factor for energy

operator is newly proposed to fulfill the combine method which means more validations are needed for the general reconstruction operator itself. The nonequilibrium scheme [15] is a valid LBM boundary condition that was reported to have the second order accuracy. This scheme is applied to obtain the density and energy distributions on the LBM zone artificial boundary using the results in FVM zone in this paper. The LBM is solving a compressible problem while FVM is based on incompressible assumption. Then a pressure based correction method is applied to transfer density from an incompressible domain to a compressible domain. Then natural convections in a squared enclosure with different Rayleigh numbers are solved using the coupled method and the results are compared with those obtained from pure LBM and pure FVM for validation of the coupled method.

2. Thermal LBM model

Two distribution functions are selected for the fluid flow and heat transfer in LBM. The density and energy distributions are represented by f_i and g_i, which are related by the buoyancy force. For the velocity field, D2Q9 model is preferred. There are nine local particle velocities on each computing node as shown in Fig. 1. These velocities are given by

$$\boldsymbol{e}_i = \begin{cases} (0,0) & i=1 \\ c(-\cos\frac{i\pi}{2}, -\sin\frac{i\pi}{2}) & i=2,3,4,5 \\ \sqrt{2}c\left(-\cos\frac{(2i+1)\pi}{4}, -\sin\frac{(2i+1)\pi}{4}\right) & i=6,7,8,9 \end{cases} \tag{1}$$

where c is the lattice speed.

The density and momentum can be obtained by

$$\rho = \sum_{i=1}^{9} f_i \tag{2}$$

$$\rho \boldsymbol{V} = \sum_{i=1}^{9} \boldsymbol{e}_i f_i \tag{3}$$

By applying BGK model to Boltzmann equation [22], the equation for density distribution, f_i, is

$$f_i(\boldsymbol{r} + \boldsymbol{e}_i\Delta t, t+\Delta t) - f_i(\boldsymbol{r}, t) = \frac{1}{\tau_v}(f_i^{eq}(\boldsymbol{r}, t) - f_i(\boldsymbol{r}, t)) + F_i, \quad i = 1, 2, \ldots 9 \tag{4}$$

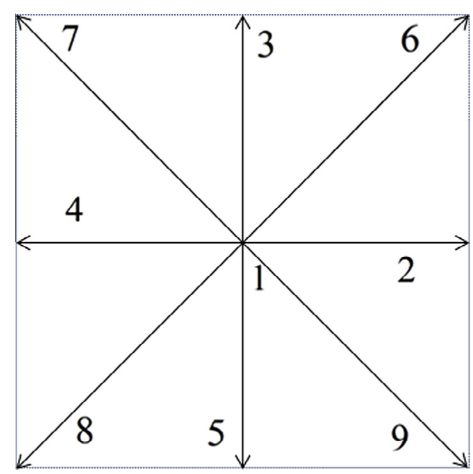

Fig. 1. Nine directions in D2Q9 model.

where Δt is the time step, and f^{eq} is the equilibrium distribution function:

$$f_i^{eq} = \rho\omega_i\left[1 + \frac{\boldsymbol{e}_i \cdot \boldsymbol{V}}{c_s^2} + \frac{(\boldsymbol{e}_i \cdot \boldsymbol{V})^2}{2c_s^4} - \frac{\boldsymbol{V}\cdot\boldsymbol{V}}{2c_s^2}\right] \tag{5}$$

where

$$\omega_i = \begin{cases} \frac{4}{9} & i=1 \\ \frac{1}{9} & i=2,3,4,5 \\ \frac{1}{36} & i=6,7,8,9 \end{cases} \tag{6}$$

Then the Navier–Stokes equation can be obtained through Chapman-Enskog expansion [16] when the kinematic viscosity ν is related to the relaxation time τ_v in Eq. (4) by:

$$\nu = c_s^2\left(\tau_v - \frac{1}{2}\right)\Delta t \tag{7}$$

where c_s is the speed of sound that is related to the lattice speed by $3c_s^2 = c^2$

The buoyancy force can be obtained as:

$$F_i = \Delta t \boldsymbol{G} \cdot \frac{(\boldsymbol{e}_i - \boldsymbol{V})}{p} f_i^{eq} \tag{8}$$

where the pressure, p, equals ρc_s^2.

The D2Q5 model [16] is used for the temperature field. There are five discrete velocity at each computing node shown is Fig. 2. Similar to the density distribution, the energy distribution can be obtained by

$$g_i(\boldsymbol{r}+\boldsymbol{e}_i\Delta t, t+\Delta t) - g_i(\boldsymbol{r},t) = \frac{1}{\tau_T}(g_i^{eq}(\boldsymbol{r},t) - g_i(\boldsymbol{r},t)), \quad i = 1,2,\ldots 5 \tag{9}$$

The macroscopic energy equation can be obtained from Eq. (9) using Chapman-Enskog expansion.

Then the relaxation time τ_T is related to the thermal diffusivity α by

$$\alpha = c_s^2\left(\tau_T - \frac{1}{2}\right)\Delta t \tag{10}$$

The equilibrium energy distribution in Eq. (9) is

$$g_i^{eq} = T\omega_i^T\left(1 + \frac{\boldsymbol{e}_i \cdot \boldsymbol{V}}{c_s^2}\right) \tag{11}$$

where:

$$\omega_i^T = \begin{cases} \frac{1}{3} & i = 1 \\ \frac{1}{6} & i = 2,3,4,5 \end{cases} \tag{12}$$

The temperature at each computing node can be obtained as:

$$T = \sum_{i=1}^{5} g_i \tag{13}$$

3. Coupled LBM-FVM method

3.1. Problem statement

Natural convection of incompressible fluid in a squared enclosure as shown in Fig. 3 is used to test the coupled method. For the velocity field, non-slip condition is applied to all boundaries. The left boundary is kept at a constant temperature T_h while the right boundary has a lower constant temperature of T_l. The top and bottom boundaries are adiabatic. Applying Boussinesq assumption, the problem can be described by the following governing equations:

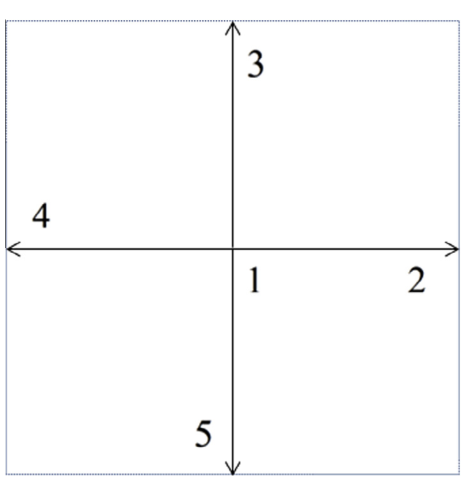

Fig. 2. Five directions in D2Q5 model.

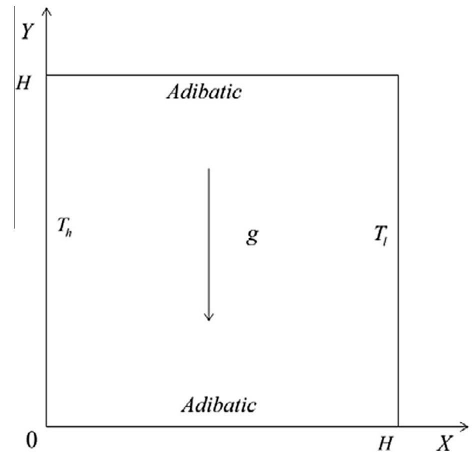

Fig. 3. Physical model of the natural convection problem.

$$\frac{\partial u}{\partial x} + \frac{\partial v}{\partial y} = 0 \tag{14}$$

$$\rho\left[\frac{\partial u}{\partial t} + u\frac{\partial u}{\partial x} + v\frac{\partial u}{\partial y}\right] = -\frac{\partial p}{\partial x} + \mu\left(\frac{\partial^2 u}{\partial x^2} + \frac{\partial^2 u}{\partial y^2}\right) \tag{15}$$

$$\rho\left[\frac{\partial v}{\partial t} + u\frac{\partial v}{\partial x} + v\frac{\partial v}{\partial y}\right] = -\frac{\partial p}{\partial y} + \mu\left(\frac{\partial^2 v}{\partial x^2} + \frac{\partial^2 v}{\partial y^2}\right) + \rho g\beta(T - T_l) \tag{16}$$

$$(\rho c_p)\left[\frac{\partial T}{\partial t} + u\frac{\partial T}{\partial x} + v\frac{\partial T}{\partial y}\right] = k\left(\frac{\partial^2 T}{\partial x^2} + \frac{\partial^2 T}{\partial y^2}\right) \tag{17}$$

Eqs. (14)–(17) are subject to the following boundary and initial conditions:

$$x = 0, u = 0, v = 0, T = T_h \tag{18}$$

$$x = H, u = 0, v = 0, T = T_l \tag{19}$$

$$y = 0, u = 0, v = 0, \partial T/\partial y = 0 \tag{20}$$

$$y = H, u = 0, v = 0, \partial T/\partial y = 0 \tag{21}$$

Regarding Eq. (8) in the view of Chapman-Enskog expansion, Eq. (16) can be obtained from the D2Q9 model in LBM when effective gravity acceleration $\boldsymbol{G}$ is defined as:

$$\boldsymbol{G} = -\beta(T - T_l)\boldsymbol{g} \tag{22}$$

where β is the volume expansion coefficient of the fluid.

SIMPLE is a well accepted FVM algorithm [17] to solve the general Navier–Stokes equation based on the control volume shown in Fig. 4. The SIMPLE algorithm with QUICK scheme [3] is employed to solve Eqs. (14)–(17). Prandtl number, Pr, and Rayleigh number, Ra, are the two non-dimensional parameters governing the natural convection.

$$Pr = \frac{\alpha}{\nu} \tag{23}$$

$$Ra = \frac{g\beta(T_h - T_l)H^3 Pr}{\nu^2} \tag{24}$$

For LBM Mach number, Ma, is needed:

$$Ma = \frac{u_c}{c_s} \tag{25}$$

where u_c is the speed of sound that equals $\sqrt{g\beta(T_h - T_l)H}$. Since the natural convection in consideration is incompressible, Ma can be any number in the incompressible region. Applying the following non-dimensional variables

$$X = \frac{x}{H}, \quad Y = \frac{y}{H}, \quad U = \frac{u}{\sqrt{3}c_s}, \quad V = \frac{v}{\sqrt{3}c_s}$$
$$\tau = \frac{t \cdot \sqrt{3}c_s}{H}, \quad \theta = \frac{T - T_l}{T_h - T_l}, \quad P = \frac{p}{3\rho c_s^2} \tag{26}$$

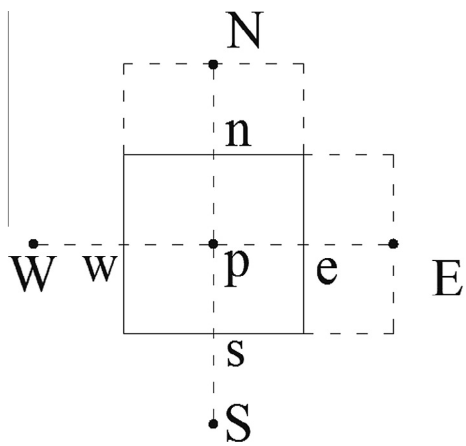

Fig. 4. Control volume in 2-D FVM.

to Eqs. (14)–(21), the dimensionless governing equations are obtained:

$$\frac{\partial U}{\partial X}+\frac{\partial V}{\partial Y}=0 \tag{27}$$

$$\frac{\partial U}{\partial \tau}+U\frac{\partial U}{\partial X}+V\frac{\partial U}{\partial Y}=-\frac{\partial P}{\partial X}+Ma\sqrt{\frac{Pr}{3Ra}}\left(\frac{\partial^2 U}{\partial X^2}+\frac{\partial^2 U}{\partial Y^2}\right) \tag{28}$$

$$\frac{\partial V}{\partial \tau}+U\frac{\partial V}{\partial X}+V\frac{\partial V}{\partial Y}=-\frac{\partial P}{\partial Y}+Ma\sqrt{\frac{Pr}{3Ra}}\left(\frac{\partial^2 V}{\partial X^2}+\frac{\partial^2 V}{\partial Y^2}\right)+\frac{Ma^2\theta}{3} \tag{29}$$

$$\frac{\partial \theta}{\partial \tau}+U\frac{\partial \theta}{\partial X}+V\frac{\partial \theta}{\partial Y}=Ma\sqrt{\frac{1}{3Ra\cdot Pr}}\left(\frac{\partial^2 \theta}{\partial X^2}+\frac{\partial^2 \theta}{\partial Y^2}\right) \tag{30}$$

For the heat transfer at the left boundary, Nusselt number, Nu, can be obtained by the nondimensional temperature gradient at the surface:

$$Nu=\left.\frac{\partial \theta}{\partial X}\right|_{X=0} \tag{31}$$

which reflects the ratio of convection to the conduction heat transfer across the wall.

3.2. Description of the coupled method

This coupled method is designed to solve a single problem with FVM and LBM simultaneously. The computational domain is divided into LBM and FVM zones, and there is a public area between these two zones. The artificial boundary of FVM zone is the inner nodes of LBM zone while the LBM artificial boundary is inside the FVM zone. Two kinds of geometry settings are applied to test this coupled method shown in Fig. 5. To fulfill the coupled method, the information on the artificial boundary needs to be obtained from the other subdomain. For the FVM zone, the velocity and temperature on the artificial boundary are needed from LBM zone. Density is not needed because FVM is solving the incompressible flow. The pressure on that boundary can be obtained directly from the FVM zone itself [3]. On the other hand, LBM needs the velocity, temperature and the density information of the artificial boundary from the FVM zone. It is not straightforward to transfer the density from an incompressible FVM zone to the compressible LBM zone. The average density in the message passing zone, ρ_0, is calculated in the message LBM zone, and the FVM zone provides the average pressure in the message passing zone, $\overline{p}$. Meanwhile, the pressure on the LBM artificial boundary, p^L, can be obtained from the FVM zone pressure, p^S. It is shown that there is very small difference between p^L and p^S in the message passing zone. But this small

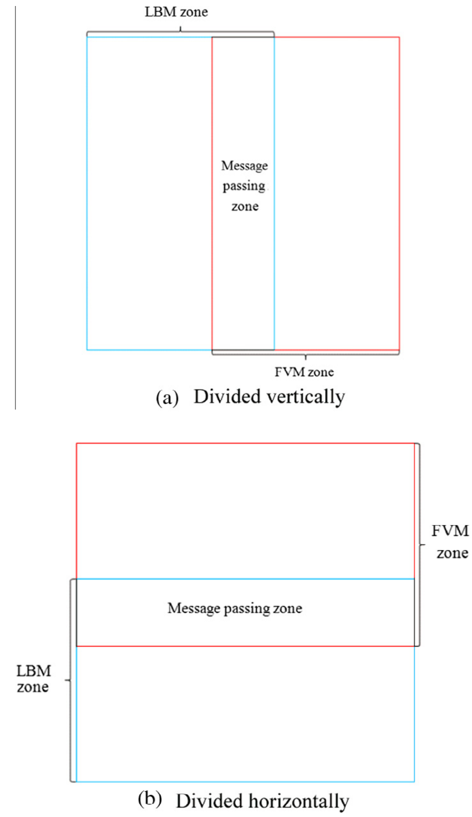

Fig. 5. Computational domains for LBM and FVM.

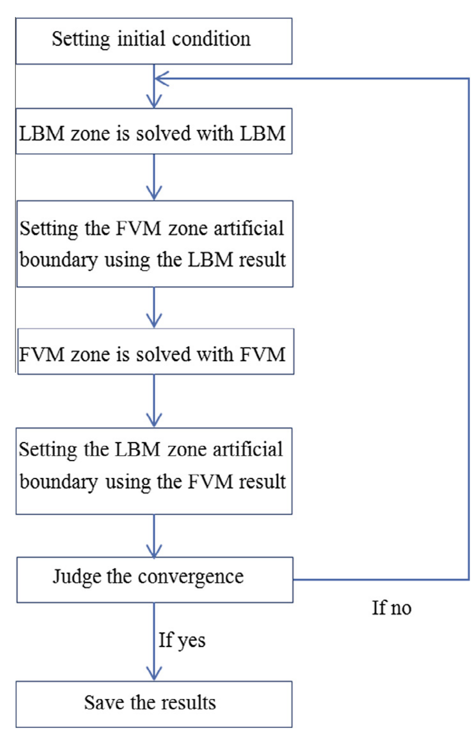

Fig. 6. Variables locations.

difference leads evident error when this coupled method is fulfilled. It is also found that the pressure gradients differences from the two methods in the message passing zone is not evident either, Thresfore, the difference between $\overline{p}^L$ and $\overline{p}$ is similar to that

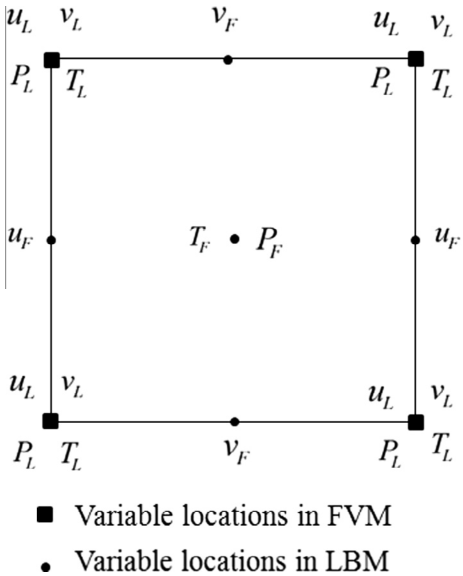

Fig. 7. Flowchart.

between p^L and p^S where $\bar{p}^L$ is average pressure in the message passing zone calculated by the LBM zone results. Thus, it is reasonable to assume that [19]:

$$p^L - \bar{p}^L = p^S - \bar{p} \tag{32}$$

Regarding the relation between pressure and density in LBM, it can be obtained that

$$\rho^L c_s^2 - \rho_0 c_s^2 = p^S - \bar{p} \tag{33}$$

Then the unknown ρ^L can be obtained that

$$\rho^L = \rho_0\left(\frac{p^S - \bar{p}}{\rho_0 c_s^2} + 1\right) \tag{34}$$

The density information on the artificial boundary of LBM can be obtained by the result of the FVM result.

Staggered grid is applied to SIMPLE algorithm. Fig. 6 shows the locations of variables in a control volume for LBM and FVM. The variables in LBM all locates on the corner of the control volume while velocity, pressure and temperature in FVM have different locations in the control volume. Central difference is applied to message passing processes due to the variable location differences.

After transferring the information from each other, the FVM and LBM zones need to be solved independently for each time step. For the FVM zone, temperatures and velocities on the four boundaries are known so that the solution procedure is straightforward. There are several choices for the LBM boundary conditions. Nonequilibrium extrapolation scheme [15] is applied to both velocity and temperature fields in the solving process. Assuming x_b is the boundary node and x_f is its nearby inner mode, the density and energy distribution at the artificial boundary are:

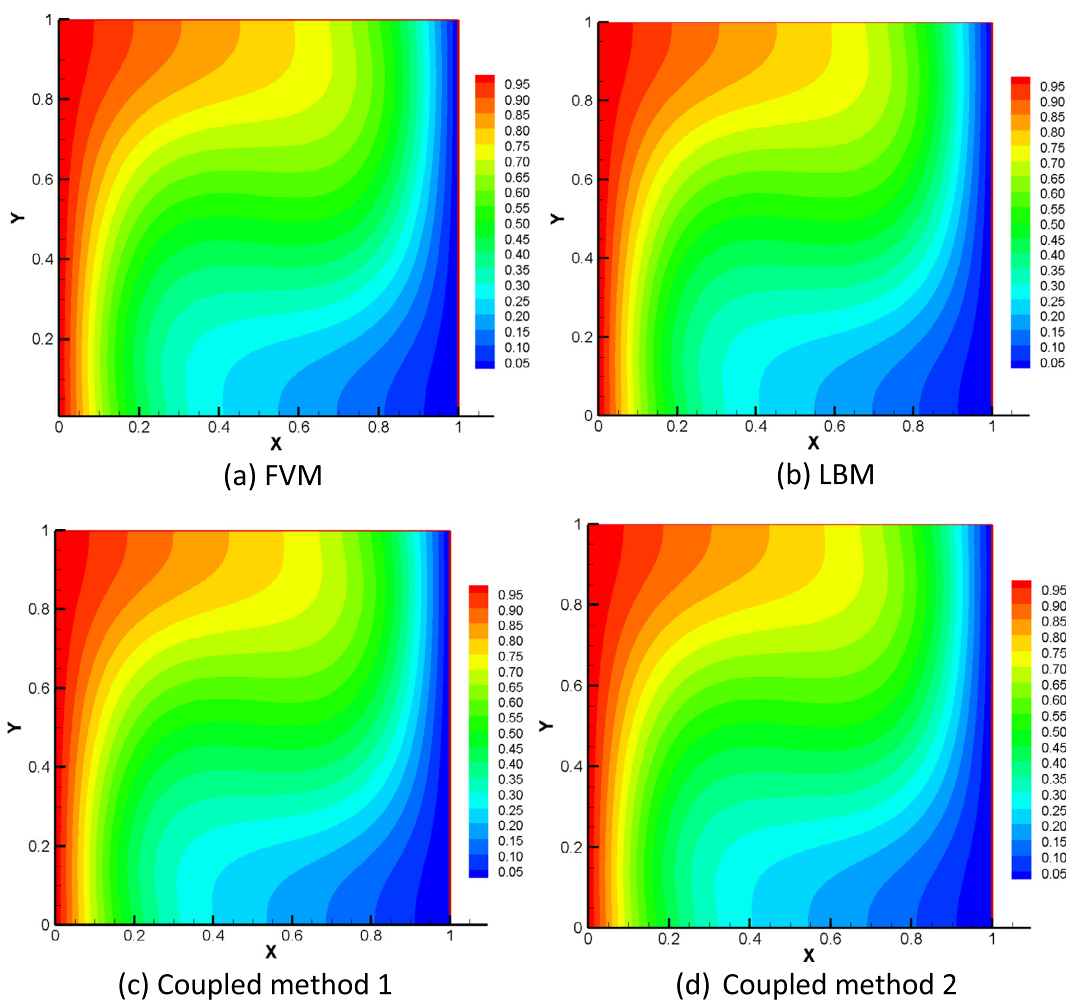

Fig. 8. Temperature fields at $Ra = 10^4$.

$$f_i(x_b,t) = f_i^{eq}(x_b,t) + f_i(x_f,t) - f_i^{eq}(x_f,t) \quad (36)$$

$$g_i(x_b,t) = g_i^{eq}(x_b,t) + g_i(x_f,t) - g_i^{eq}(x_f,t) \quad (37)$$

The temperatures on the boundaries are known in every time step, Eq. (37) can be applied to the thermal boundary conditions for Eq. (11). For the velocity field, the boundary density is only known on the artificial boundary. It is common to approximate the density on the fixed boundary by

$$\rho(x_b,t) = \rho(x_f,t) \quad (38)$$

Fig. 7 shows the flowchart of the computational procedure for the coupled method.

4. Results and discussion

Natural convection in a squared enclosure is solved for three different Rayleigh numbers at 10^4, 10^5 and 10^6 while the Prantl number is kept at 0.71. Pure LBM and pure FVM are reported in the literature to be suitable for the natural convection in a cavity. Thus, these two methods are applied to solve the test cases. If the LBM results agree with the FVM results, it can be concluded that these results can be used as standard results for comparison. It can also verify that the codes for the two subdomains are reliable in the coupled method. Then only the message passing method between the two subdomains affects the results from the coupled

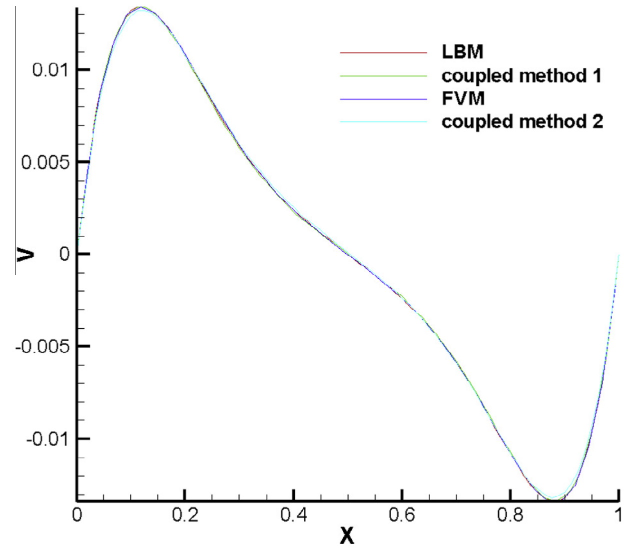

Fig. 10. .Vertical velocity comparison on the centerline of cavity at $Ra = 10^4$.

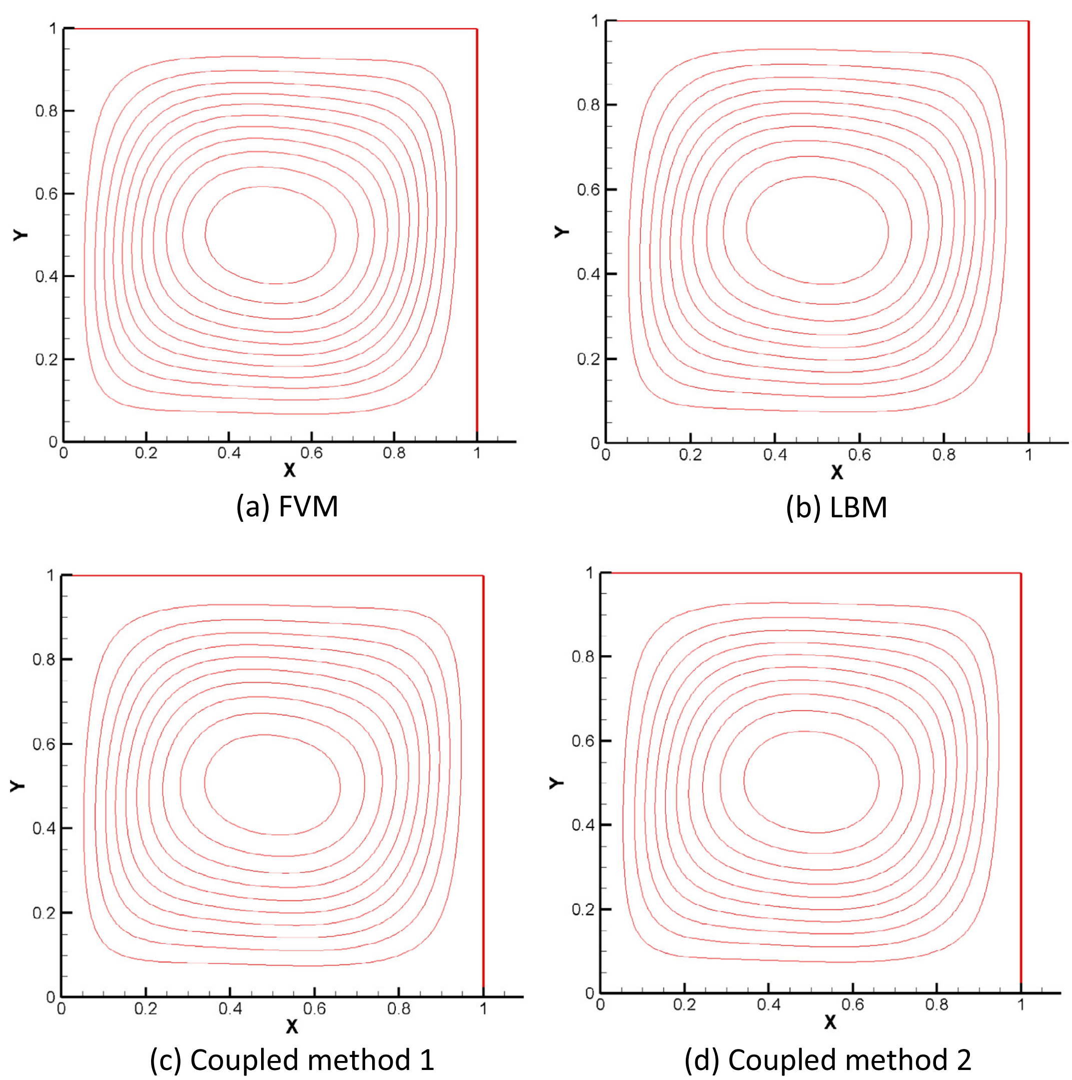

Fig. 9. Streamlines at $Ra = 10^4$.

methods. Two coupled methods with different geometry settings are applied. When the domain is divided vertically, it is referred to as Coupled Method 1. And the Coupled Method 2 divides the domain horizontally as shown in Fig. 5. Temperature field, streamline, vertical velocity on the centerline of cavity and Nusselt number on the left wall obtained from these four methods are compared for the three cases. Nondimensional variables defined in Eq. (26) are applied in the comparisons.

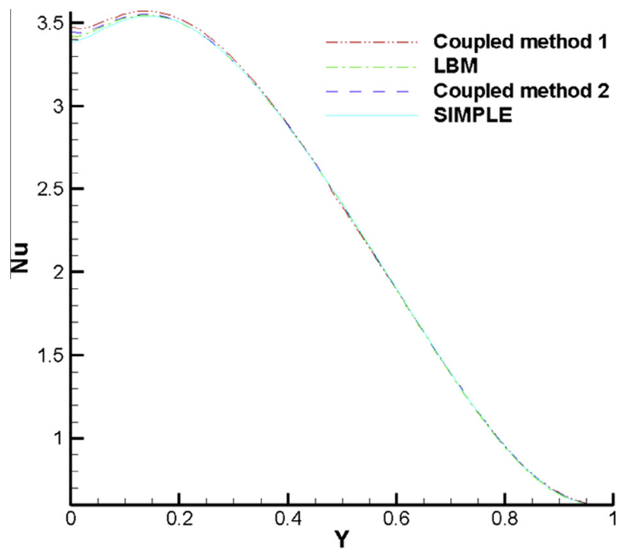

Fig. 11. Nusselt numbers at $Ra = 10^4$.

Figs. 8 and 9 show comparisons of temperature field and streamlines obtained by different methods for the case that Rayleigh number is 10^4. It is obvious that natural convection has dominated the heat transfer process and there is a stream line vertex near the center of the cavity. Temperature fields and streamlines obtained from pure LBM and pure FVM agree with each other well as shown in Figs. 8 and 9. In addition, there is not any noticeable difference between the results obtained from coupled methods 1 and 2 and the results of coupled methods agreed with that from the pure FVM and pure LBM very well. Figs. 10 and 11 show the vertical velocity on the centerline of cavity and Nusselt number at heated wall along the vertical direction of the enclosure obtained from different methods. There is a little difference between the vertical velocity and Nusselt numbers obtained from pure LBM and pure FVM. The cause of this difference is that FVM is based on the incompressible fluid assumption while LBM is based on compressible fluid assumption. Meanwhile the vertical velocity and Nusselt number tendencies of the two coupled methods are very close to that of the two pure methods.

Figs. 12 and 13 show the temperature field and streamlines obtained by different methods for the case that Rayleigh number is 10^5. It can be see that the pure FVM and pure LBM reach similar temperature fields and streamlines. The convection effect becomes more pronounced as the Rayleigh number increases.

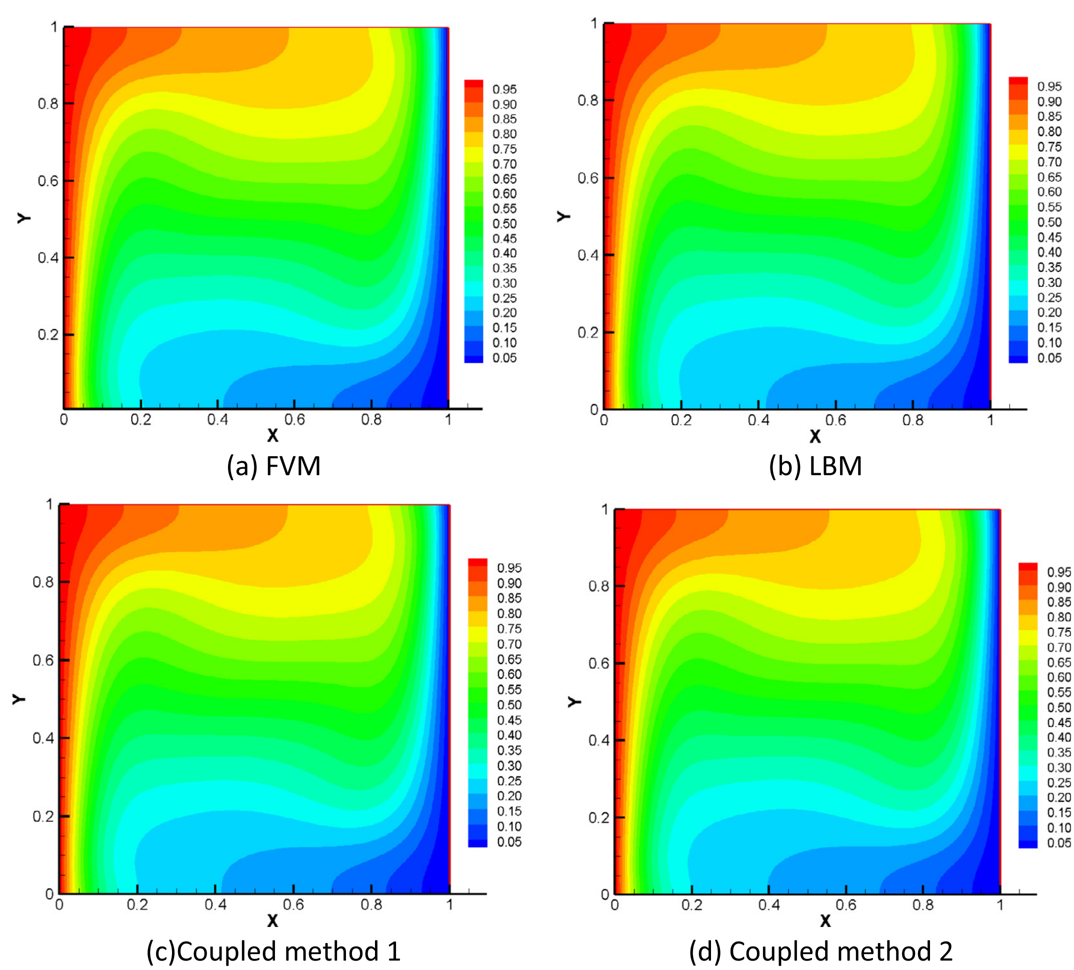

Fig. 12. Temperature fields at $Ra = 10^5$.

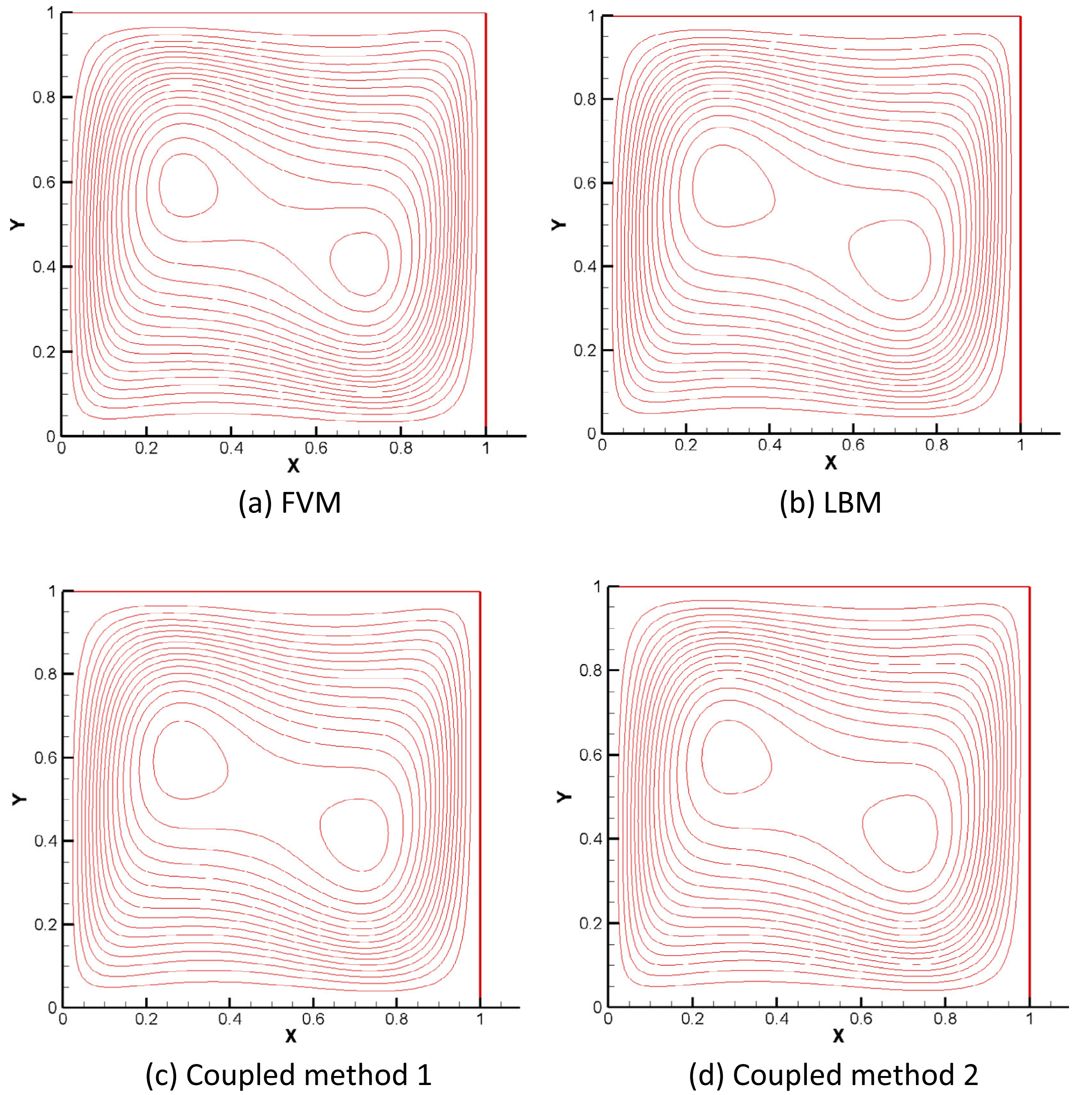

Fig. 13. Streamlines at $Ra = 10^5$.

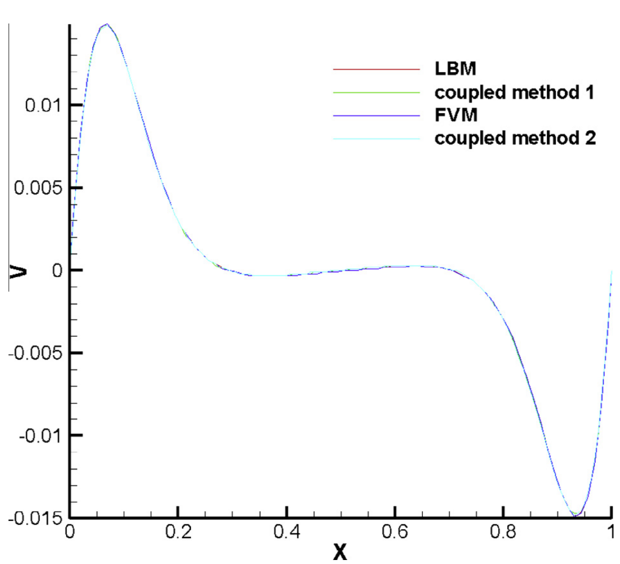

Fig. 14. Vertical velocity comparison on the centerline of cavity at $Ra = 10^5$.

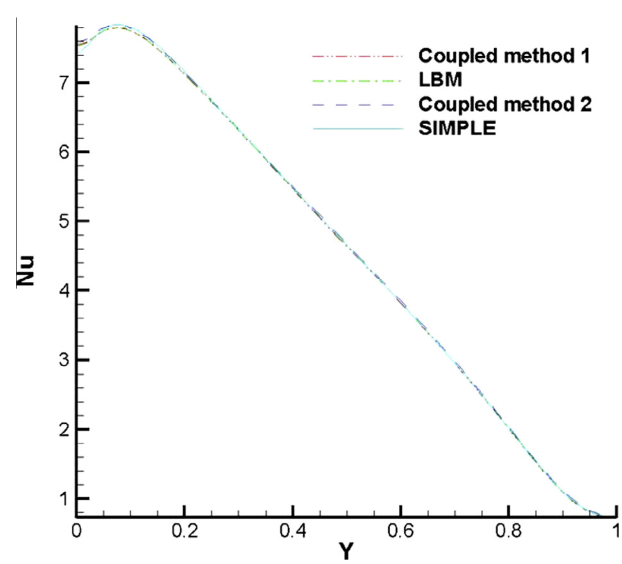

Fig. 15. Nusselt numbers at $Ra = 10^5$.

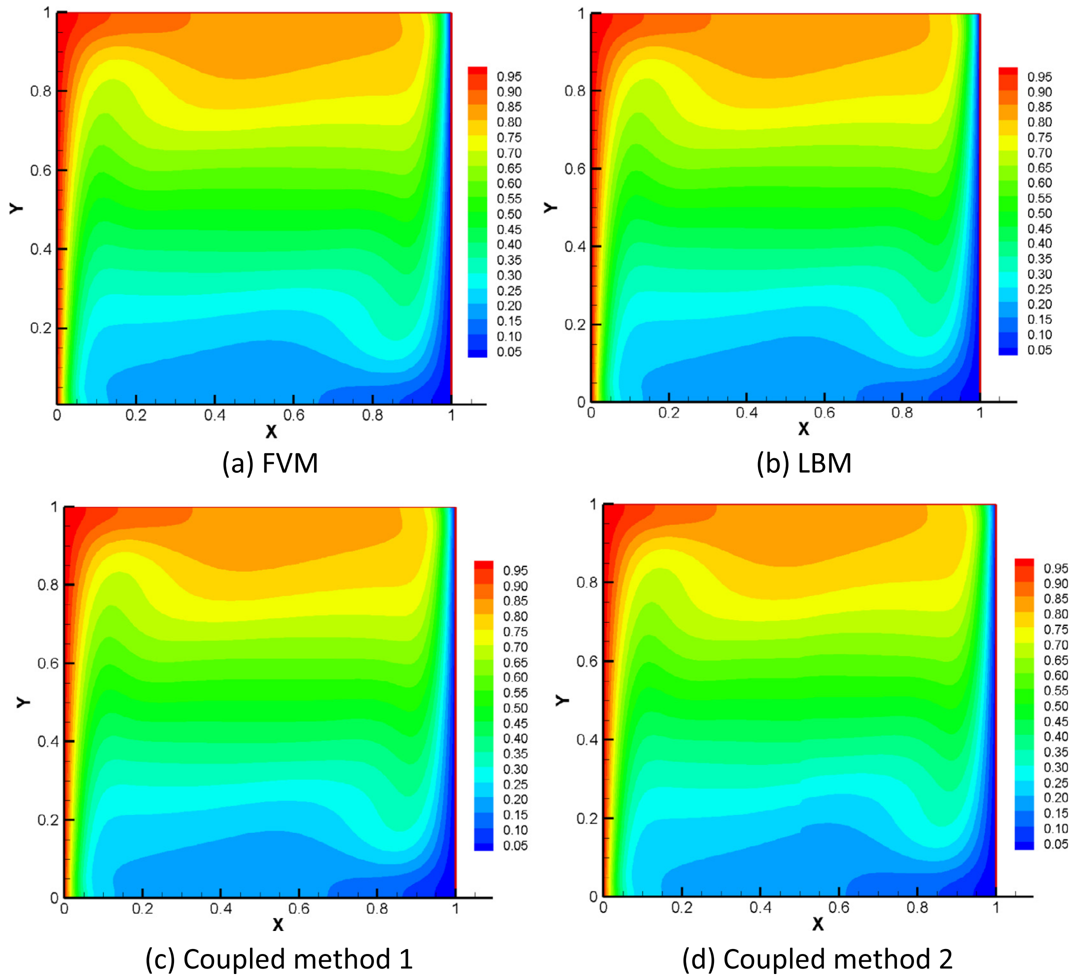

Fig. 16. Temperature fields at $Ra = 10^6$.

Two vertexes appear and the temperature gradients near the vertical boundary increase. The two coupled method results still agree very well with that in the pure methods as shown in Figs. 12 and 13. For the centerline vertical velocity comparison shown in the Fig. 14, it is very hard to find the difference between each other. Coupled methods results agree with the pure methods results very well. Meanwhile, Fig. 15 shows that the difference between Nusselt numbers obtained from pure FVM and pure LBM is larger than that in Fig. 11; but the largest difference is still round 2%. The Nusselt numbers from the two coupled methods are closer to the results of pure LBM than that of the pure FVM. Since both coupled methods 1 and 2 have half regions with LBM that do not have incompressible fluid assumption, the fluid in the entire computational domain of the coupled methods can be considered as compressible. The Nusselt number differences between the two coupled methods are not larger than that between the two pure methods.

Convection continues to become stronger when Rayleigh number is increased to 10^6. Figs. 16 and 17 show that all four methods yield the similar temperature fields and streamlines. There are still two independent stream line vertexes that are closer to the vertical boundaries; this indicates a stronger convection effect comparing with the results when Rayleigh number is 10^5. As for the centerline vertical velocity and Nusselt number, Figs. 18 and 19 show that the results from the coupled methods 1 and 2 are very close to that from the pure LBM. And the differences between the two coupled methods and pure FVM are still acceptable.

The results obtained by the coupled methods 1 and 2 are as good as those from the pure FVM and pure LBM in all the three cases. The time consumption for the coupled method is higher than that of the pure FVM but lower than that of pure LBM. Comparing to FVM, LBM can show its advantage when solving the fluid flow and heat transfer problem in the complex geometry. Therefore FVM is the most suitable method for the natural convection in the cavity discussed above. Meanwhile the fluid flow and heat transfer problem in reality does not always have the regular geometry. For the cases that involve complex geometry as part of the computational; domain, the coupled methods discussed above will be more suitable than both pure FVM and pure LBM.

5. Conclusion

A coupled LBM and FVM method is proposed for the fluid heat transfer problem. Nonequilibrium extrapolation scheme is used to couple the macroscopic variables in FVM region to the mesoscopic variables in LBM region. Two coupled methods with different geometric settings are employed to solve the natural convection in a squared enclosure and the results are compared with that obtained from pure FVM and LBM. The results obtained from the four methods agreed with each other very well at different Rayleigh numbers of 10^4, 10^5 and 10^6. The geometric settings do not affect the accuracy of the coupled method. The results of this work demonstrated that the coupled method is reliable to solve natural convection problems.

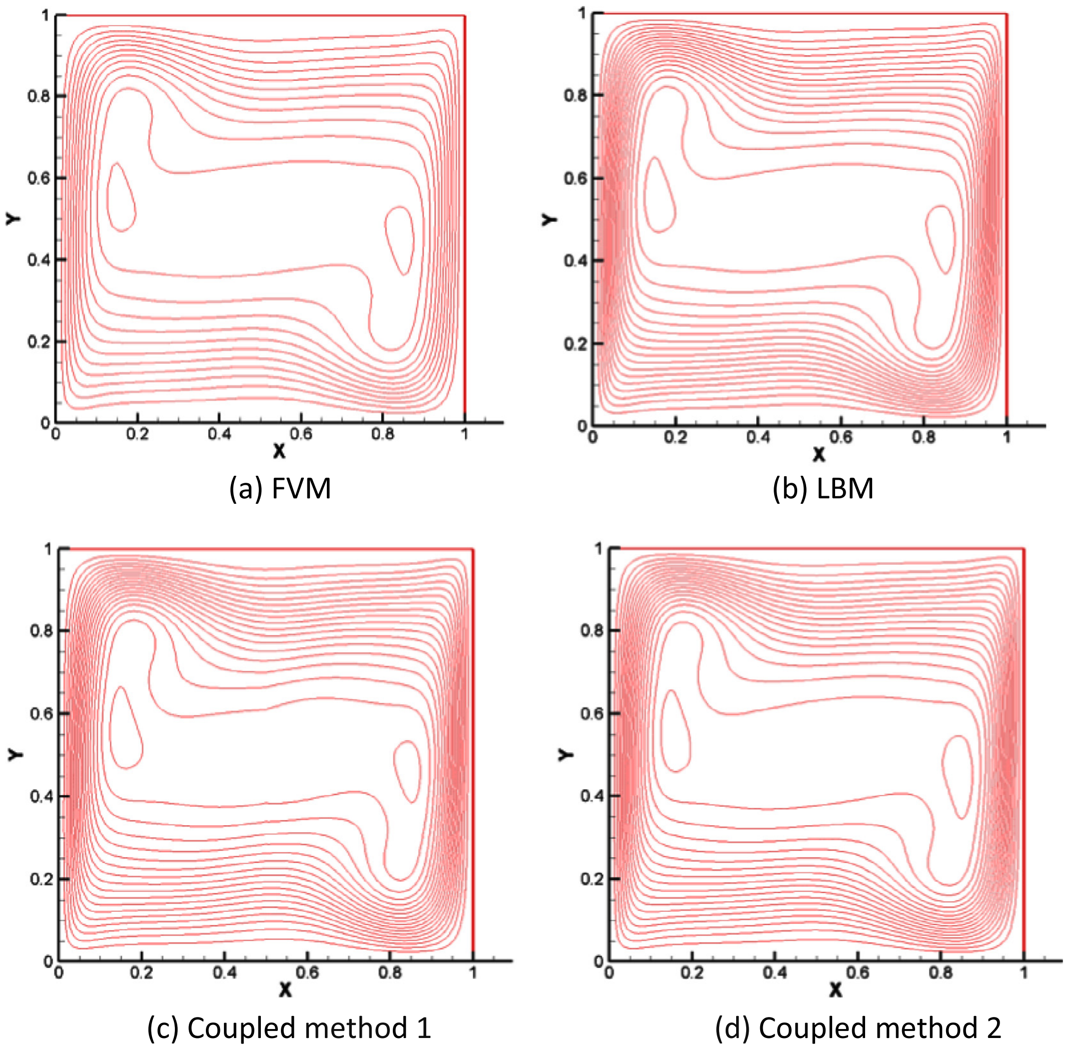

Fig. 17. Streamlines at $Ra = 10^6$.

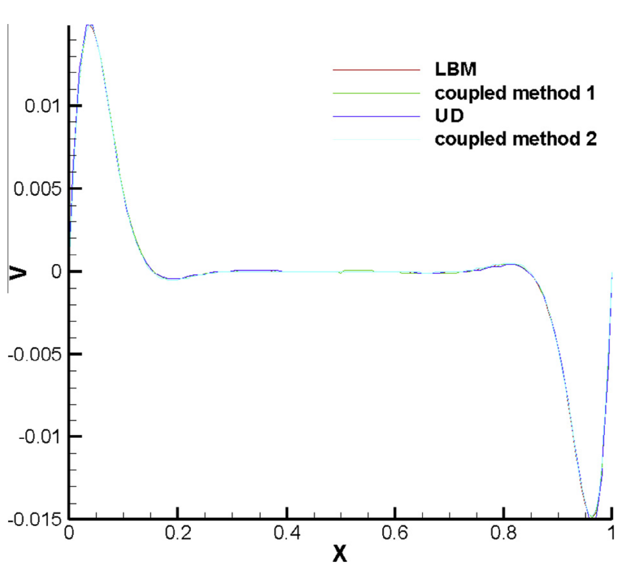

Fig. 18. Vertical velocity comparison on the centerline of cavity at $Ra = 10^6$.

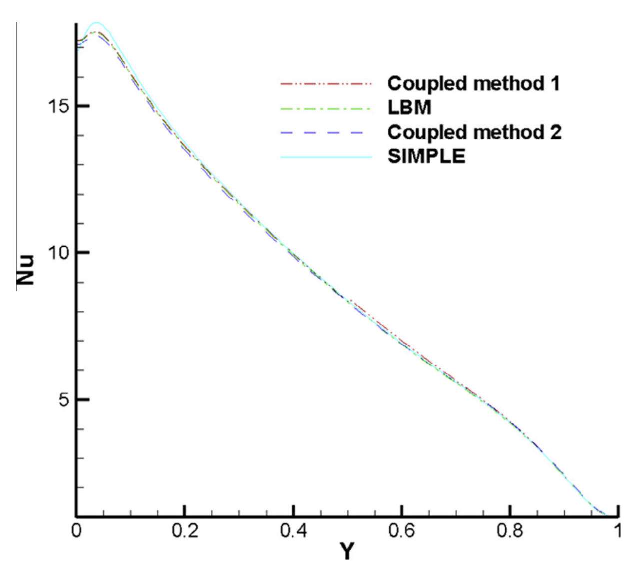

Fig. 19. Nusselt numbers at $Ra = 10^6$.

Acknowledgment

Support for this work by the U.S. National Science Foundation under grant number CBET-1066917 and Chinese National Natural Science Foundation under Grants 51129602 and 51276118 is gratefully acknowledged.

References

[1] G. Grest, K. Kremer, Molecular dynamics simulation for polymers in the presence of a heat bath, Phys. Rev. A 33 (1986) 3628–3631.
[2] S. Succi, Lattice Boltzmann Method for Fluid Dynamics and Beyond, Oxford University Press, 2001.
[3] W.Q. Tao, Numerical Heat Transfer, Xi'an Jiaotong University Press, Xi'an, 2001.
[4] T. Werder, J. Walther, P. Koumout, Hybrid atomistic-continuum method for the simulation of dense fluid flows, J. Comput. Phys. 205 (1) (2005) 373–390.
[5] A. Dupuis, E. Kotsalis, P. Koumoutsakos, Coupling lattice Boltzmann and molecular dynamics models for dense fluids, Phys. Rev. E 75 (2007) 046704.
[6] D. Fedosov, G. Karniadakis, Triple-decker, Interfacing atomistic–mesoscopic–continuum flow regimes, J. Comput. Phys. 228 (4) (2009) 1157–1171.
[7] S. O'Connell, P. Thompson, Molecular dynamics-continuum hybrid computations: A tool for studying complex fluid flows, Phys. Rev. E 52 (1995) R5792–R5795.
[8] E. Flekkoy, G. Wagner, J. Feder, Hybrid model for combined particle and continuum dynamics, Europhys. Lett. 52 (2000) 271–276.
[9] X. Nie, S. Chen, A continuum and molecular dynamics hybrid method for micro- and nano-fluid flow, J. Fluid Mech. 500 (2004) 55–64.
[10] B. Mondal, S. Mishra, Lattice Boltzmann method applied to the solution of the energy equations of the transient conduction and radiation problems on non-uniform lattices, Int. J. Heat Mass Transfer 51 (2008) 68–82.
[11] B. Mondal, S. Mishra, The lattice Boltzmann method and the finite volume method applied to conduction–radiation problems with heat flux boundary conditions, Int. J. Numer. Methods Eng. 78 (2) (2009) 172–195.
[12] H. Joshi, A. Agarwal, B. Puranik, C. Shu, A hybrid FVM–LBM method for single and multi-fluid compressible flow problems, Int. J. Numer. Methods Fluids 62 (2010) 403–427.
[13] X. He, S. Chen, G. Doolen, A novel thermal model for the lattice Boltzmann method in incompressible limit, J. Comput. Phys. 146 (1998) 282–300.
[14] Y. Peng, C. Shu, Y. Chew, Simplified thermal lattice Boltzmann model for incompressible thermal flows, Phys. Rev. E 68 (2003) 026701.
[15] Z. Guo, B. Shi, C. Zheng, A coupled lattice BGK model for the Boussinesq equations, Int. J. Numer. Methods Fluids 39 (2002) 325–342.
[16] C. Huber, A. Parmigiani, B. Chopard, M. Manga, O. Bachmann, Lattice Boltzmann model for melting with natural convection, Int. J. Heat Fluid Flow 29 (2008) 1469–1480.
[17] S.V. Patankar, Numerical Heat Transfer and Fluid Flow, McGraw-Hill Book Co., 1980.
[18] J. Latt, Hydrodynamic Limit of Lattice Boltzmann Equations, Ph.D. Thesis, University of Geneva, 2007.
[19] J. Latt, B. Chopard, P. Albuquerque, Spatial coupling of a lattice Boltzmann fluid model with a finite difference Navier–Stokes solver, Technical Report, Cornell University, 2008.
[20] H. Luan, H. Xu, L. Chen, Coupling of finite volume method and thermal lattice Boltzmann method and its application to natural convection, Int. J. Numer. Methods Fluids 70 (2012) 200–221.
[21] H. Luan, H. Xu, L. Chen, Evaluation of the coupling scheme of FVM and LBM for fluid flows around complex geometries, Int. J. Heat Mass Transfer 54 (2011) 1975–1985.
[22] S. Chen, G. Doolen, Lattice Boltzmann method for fluid flows, Annu. Rev. Fluid Mech. 30 (1998) 329–364.